

Article ID: 1006-8775(2015) S1-0066-0

THE LOW-PRESSURE SYSTEM IN THE VERTICAL VELOCITY OMEGA ON THE SCALE OF SYSTEM SENSITIVITY

QU Wei-zheng (曲维政), FAN Ting-ting (范婷婷), DU Ling (杜凌)

(College of Physical and Environmental Oceanography, Ocean University of China, Qingdao 266041 China)

Abstract: In this study, the relationship between scale and vertical velocity in a low-pressure system is explored using the wave characteristics of atmospheric disturbances and the structural characteristics of low-pressure systems. The ω differential equation, as determined by the transient geopotential height field Φ , is solved to obtain an analytical solution composed only of wavelength, horizontal speed, and atmospheric stability, i.e., the ω diagnostic equation of a low-pressure system. This equation also shows that vertical velocity in the low-pressure system is very sensitive to the horizontal scale, i.e., a smaller horizontal scale means a larger vertical velocity.

Key words: vertical speed; wave length; wind speed; static stability; low-pressure system; vortex; diagnostic analysis

CLC number: P456 **Document code:** A
doi: 10.16555/j.1006-8775.2015.S1.007

1 INTRODUCTION

Existing methods for the calculation of vertical velocity (Zhang^[1]; Lv et al.^[2]; Xu et al.^[3]; Chu et al.^[4]; Song et al.^[5]; Zheng and Xue^[6]; Kuai et al.^[7]; Alexander and Wurman^[8]) are unsuitable for timely and effective diagnoses of sudden small-scale weather systems, e.g., tornadoes. Therefore, in this study, the geopotential field Φ and vertical velocity ω are substituted into appropriate equations via Fourier series expansion according to the wave characteristics of the atmospheric disturbance. Using operations such as the Laplace equation and P differential, a concise ω diagnostic equation is obtained. This equation shows that in terms of stability, ω is determined only by wavelength (or wave number) and wind speed, i.e., ω is positively correlated with wind speed but negatively correlated with wavelength. Thus, the derived equation greatly simplifies the process of diagnosing vertical speed. Because the methods for calculating vertical velocity vary greatly, in order to distinguish them, this equation is referred to as the ω diagnostic equation of low-pressure systems.

2 Ω DIAGNOSTIC EQUATION OF LOW-PRESSURE SYSTEMS

As a small-scale atmospheric vortex, a low-pressure system is a violently rotating vortex of strong winds with severe convective motion forming a condensation funnel, which occurs under conditions of extreme atmospheric instability. The horizontal scale of such low-pressure systems is very small. Typically, the radius varies from several to several hundred meters (maximum around 1 000 m) with an average radius of around 250 m^[2].

For the case of the onset of the vortex, the derivation of the ω diagnostic equation is straightforward; however, further analysis requires specific discussion depending on the characteristics of the low-pressure system. The vorticity equation for the determination of the vertical component of vorticity ζ_p is shown below:

$$\frac{\partial \zeta_p}{\partial t} = -\vec{V} \cdot \nabla (\zeta_p + f) - \omega \frac{\partial \zeta_p}{\partial p} - (\zeta_p + f) \nabla_p \cdot \vec{V} + \left(\frac{\partial u}{\partial p} \frac{\partial \omega}{\partial y} - \frac{\partial v}{\partial p} \frac{\partial \omega}{\partial x} \right)$$

For synoptic-, meso-, and small-scale motions, the second term of vorticity convection and the final term

Received 2014-12-17; **Revised** 2015-08-07; **Accepted** 2015-09-15

Foundation item: National Science Foundation of China: Arctic Sea Ice and the Coupling of the Upper Ocean Circulation Changes and Climate Effect (41376008, 41330960)

Biography: QU Wei-zheng, Professor, primarily undertaking research on abnormal climate change.

Corresponding author: QU Wei-zheng, e-mail: quweizhe@ouc.edu.cn

of the twisting term on the right-hand side of this equation are negligible. In the divergence term, ζ_p is less than f ; hence, ζ_p is negligible. The relative vorticity can be substituted by the relative vorticity of the geostrophic wind, which gives the following:

$$\frac{\partial \zeta_g}{\partial t} = -\vec{V} \cdot \nabla_p (\zeta_g + f) - f \nabla_p \cdot \vec{V}$$

The continuity equation $\nabla_p \cdot \vec{V} = -\frac{\partial \omega}{\partial p}$ and the

formula $\zeta_g = \frac{\nabla_p^2 \phi}{f}$ can be used to transform the equation as

$$\frac{\partial}{\partial p} (\nabla_p^2 \frac{\partial \phi}{\partial t}) = -f \frac{\partial}{\partial p} \left[\vec{V} \cdot \nabla_p \left(\frac{\nabla_p^2 \phi}{f} + f \right) \right] + f^2 \frac{\partial^2 \omega}{\partial p^2}$$

Subtracting the two equations and exchanging the P differential and Laplace operator gives

$$\left(\nabla_p^2 + \frac{f^2}{\sigma_s} \frac{\partial^2}{\partial p^2} \right) \omega = \frac{f}{\sigma_s} \frac{\partial}{\partial p} \left[\vec{V} \cdot \nabla_p \left(\frac{\nabla_p^2 \phi}{f} + f \right) \right] + \frac{1}{\sigma_s} \nabla_p^2 \left[\vec{V} \cdot \nabla_p \left(-\frac{\partial \phi}{\partial p} \right) \right] \quad (3)$$

The derived equation is a diagnostic equation (known as the ω equation) in which the transient geopotential field Φ determines ω . In the equation

$\chi = \frac{\partial \phi}{\partial t}$ is the potential tendency (or heightening),

\vec{V} is the wind speed, P is the air pressure, f is the Coriolis parameter (magnitude: 10^{-5}s^{-1}), and

$\sigma_s = -\frac{\alpha}{\theta} \frac{\partial \theta}{\partial p}$ is the static stability parameter

(magnitude: around 10^{-1}).

For a wave disturbance, the distribution of the geopotential field Φ and ω can be developed to the sine (cosine) function of x and y (Chu et al.^[4]). The following is assumed:

$$\phi = \phi(p) \sin kx \sin my \quad (4)$$

$$\omega = \omega(p) \sin kx \sin my \quad (5)$$

Since a phase difference exists in the geopotential field between the upper level of 100 hPa and the lower level of 1000 hPa (the difference is 180°), the ω distribution also exhibits the same phase difference. Therefore, the following is assumed to be true:

$$\phi = A \sin \left(kx - 10 \frac{p\pi}{p_0} \right) \sin my \quad (6)$$

$$\nabla_p^2 \frac{\partial \phi}{\partial t} = -f \vec{V} \cdot \nabla_p \left(\frac{\nabla_p^2 \phi}{f} + f \right) + f^2 \frac{\partial \omega}{\partial p} \quad (1)$$

The thermodynamic equation in which the isotonic heat rate is omitted is shown below:

$$\frac{\partial}{\partial p} \left(\frac{\partial \phi}{\partial t} \right) = -\vec{V} \cdot \nabla_p \left(\frac{\partial \phi}{\partial p} \right) - \sigma_s \omega \quad (2)$$

The thermodynamic equation can be processed using the Laplace operator to obtain the following:

$$\nabla_p^2 \frac{\partial}{\partial p} \left(\frac{\partial \phi}{\partial t} \right) = -\nabla_p^2 \left[\vec{V} \cdot \nabla_p \left(\frac{\partial \phi}{\partial p} \right) \right] - \sigma_s \nabla_p^2 \omega$$

Then, the vorticity equation (Eq.1) can be operated on using the P differential to obtain

$$\omega = A \sin \left(kx - 10 \frac{p\pi}{p_0} \right) \sin my \quad (7)$$

These equations are equivalent to the geopotential height field and vertical velocity ω distributed on the 100-hPa isobaric surface for which the phase difference is 180° in comparison with that at sea level. In the Fourier series expansion equation, k is the wave number, which is equivalent to $2\pi/L_x$ (L_x is the wavelength in the x direction), m is the wave number in the y direction, which is equivalent to $2\pi/L_y$ (L_y is the wavelength in the y direction). If Eqs. (5) and (7) in the above Fourier series expansion are substituted into the left-hand side of Eq.(3), the Laplace operator used, and the P differential calculated, the result is given by

$$\left(\nabla_p^2 + \frac{f^2}{\sigma_s} \frac{\partial^2}{\partial p^2} \right) \omega = - \left[k^2 + m^2 + \frac{1}{\sigma_s} \left(\frac{10f\pi}{p_0} \right)^2 \right] \omega \quad (8)$$

The left-hand side of the ω equation is proportional to $-\omega$, and the first term on the right-hand side of Eq.(3) is the differential vorticity advection. Next, Eq.(4) is substituted into the expression for geostrophic vorticity:

$$\zeta_g = \frac{1}{f} \nabla_p^2 \phi = -\frac{k^2 + m^2}{f} \phi \quad (9)$$

following which Eqs. (9) and (6) are substituted into the first and second terms, respectively, on the right-hand side of Eq.(3), and the corresponding operations are conducted.

Low-pressure systems occur mainly in the space between the base of severe thunderclouds and the ground. Hence, their vertical extent is usually insubstantial, and the vertical shear level of the low-pressure system speed is relatively low, which means that speed can be considered constant in the vertical direction. In the horizontal direction, the distance from the center of the low-pressure system to

the outside is quite small, the wind speed is high, and the airflow rotates around the central axis; therefore, the horizontal shear level of the surrounding low-pressure system speed is quite low.

This study focuses on the analysis of the vertical velocity formed by surface wind convergence. For simplicity, horizontal shear is neglected, but the average horizontal speed is given as follows:

$$\begin{aligned} \frac{f}{\sigma_s} \frac{\partial}{\partial p} \left[\vec{V} \cdot \nabla_p \left(\frac{\nabla_p^2 \phi}{f} + f \right) \right] &= \frac{f}{\sigma_s} \left[\vec{V} \cdot \nabla_p \left(\frac{k^2 + m^2}{f} \frac{10\pi}{p_0} A \cos \left(kx - \frac{10\pi p}{p_0} \right) \sin my \right) \right] \\ &= \frac{f}{\sigma_s} V \frac{k^2 + m^2}{f} \frac{10\pi}{p_0} \left[-kA \sin \left(kx - \frac{10\pi p}{p_0} \right) \sin my + mA \cos \left(kx - \frac{10\pi p}{p_0} \right) \cos my \right] \\ &= \frac{k^2 + m^2}{\sigma_s} \frac{10\pi}{p_0} V \left[-k\phi + mA \cos \left(kx - \frac{10\pi p}{p_0} \right) \cos my \right] \quad (10) \end{aligned}$$

$$\begin{aligned} \frac{1}{\sigma_s} \nabla_p^2 (\vec{V} \cdot \nabla_p (-\frac{\partial \phi}{\partial p})) &= \frac{1}{\sigma_s} \nabla_p^2 \left[\vec{V} \cdot \nabla_p \left(\frac{10\pi}{p_0} A \cos \left(kx - \frac{10\pi p}{p_0} \right) \sin my \right) \right] \\ &= \frac{1}{\sigma_s} \nabla_p^2 \left[V \frac{10\pi}{p_0} \left(-k\phi + mA \cos \left(kx - \frac{10\pi p}{p_0} \right) \cos my \right) \right] \\ &= \frac{1}{\sigma_s} \frac{10\pi}{p_0} V \left[-k(k^2 + m^2) - mA k^2 \cos \left(kx - \frac{10\pi p}{p_0} \right) \cos my (k^2 + m^2) \right] \\ &= \frac{1}{\sigma_s} \frac{10\pi}{p_0} V (k^2 + m^2) \left[-k - mA \cos \left(kx - \frac{10\pi p}{p_0} \right) \cos my \right] \quad (11) \end{aligned}$$

If Eqs.(8), (10), and (11) are substituted into Eq.(3), we get

$$\begin{aligned} - \left[k^2 + m^2 + \frac{1}{\sigma_s} \left(\frac{f\pi}{p_0} \right)^2 \right] \omega &= \frac{k^2 + m^2}{\sigma_s} \frac{10\pi}{p_0} V \left(-k\phi + mA \cos \left(kx - \frac{10\pi p}{p_0} \right) \cos my \right) \\ &+ \frac{10\pi V}{\sigma_s p_0} (k^2 + m^2) \left[-k - mA \cos \left(kx - \frac{10\pi p}{p_0} \right) \cos my \right] \\ &= - \frac{10\pi k}{p_0 \sigma_s} (k^2 + m^2) (1 + \omega) V \\ &= - \frac{10\pi k}{p_0 \sigma_s} (k^2 + m^2) V - \frac{10\pi k}{p_0 \sigma_s} (k^2 + m^2) V \omega \quad (12) \end{aligned}$$

Then, transposing the terms, combining similar terms, and sorting them means that Eq.(12) can be expressed as follows:

$$\frac{\omega}{1 + \omega} = \frac{\frac{10\pi k}{p_0 \sigma_s} (k^2 + m^2)}{k^2 + m^2 + \frac{1}{\sigma_s} \left(\frac{10f\pi}{p_0} \right)^2} V = \frac{10k\pi}{p_0 \sigma_s + \frac{10^2 f^2 \pi^2}{p_0 (k^2 + m^2)}} V \quad (13)$$

From $O(p_0 \sigma_s) = 10^3 10^{-1} = 10^2$, $O\left(\frac{10^2 f^2 \pi^2}{p_0 (k^2 + m^2)}\right) = \frac{10^2 \cdot 10^{-5} \cdot 10^1}{10^3 \cdot 10^1} = 10^{-6}$,

we obtain $p_0 \sigma_s \gg \frac{10^2 + \pi^2}{p_0 (k^2 + m^2)}$ such

above equation, we get

$$\frac{\omega}{1 + \omega} = 0.00314 \frac{k}{\sigma_s} V \quad (15)$$

that Eq.(13) can be expressed with high accuracy:

$$\frac{\omega}{1 + \omega} = \frac{\pi k}{\sigma_s p_0} V \quad (14)$$

Alternatively, $K = 2\pi/L_x$ can be substituted into Eq.(15); hence, Eq.(15) can be expressed as

By substituting $\pi = 3.14$ and $P_0 = 850$ hPa into the

$$\frac{\omega}{1 + \omega} = 0.02527 \frac{V}{L_x \sigma_s} \quad (16)$$

This means that a simplified ω diagnostic equation (Eq.(15) or (16)) can be obtained. From these equations, we know that vertical velocity ω is determined by the zonal wave number K (or wavelength L_x), static stability σ_s , and wind speed \vec{V} :

(1) When the wavelength (wave number) and atmospheric stability are constant, vertical speed ω will be determined by wind speed, meaning vertical speed ω increases with increasing wind speed and decreases with decreasing wind speed.

(2) When wind speed and atmospheric stability are constant, vertical speed ω decreases with increasing wavelength (K decreases in size) and increases with decreasing wavelength.

(3) When the wavelength (wave number) and wind speed are constant, vertical velocity ω is determined by atmospheric stability. Stability is determined according to the following condition:

$$\begin{aligned} < 0 & \text{ Stability} \\ \frac{\partial \theta}{\partial p} = 0 & \text{ Neutrality} \\ > 0 & \text{ Instability} \end{aligned}$$

$$\text{On the basis of the expression } \sigma_s = -\frac{\alpha}{\theta} \frac{\partial \theta}{\partial p},$$

the following condition results:

$$\begin{aligned} < 0 & \text{ Instability} \\ \sigma_s = 0 & \text{ Neutrality} \\ > 0 & \text{ Stability} \end{aligned}$$

When the atmosphere exhibits static stability, i.e., $\sigma_s > 0$, vertical velocity ω is positive and downdraft motion prevails, whereas when it exhibits static instability, i.e., $\sigma_s < 0$, ω is negative and updraft motion prevails. The speed of the downdraft or updraft is determined by wind speed, wavelength, and stability. As seen from Eq.(15), it is a singular point in the case of $\sigma_s = 0$. In fact, it is highly unlikely that the atmosphere will be neutral, and in order to avoid this situation, $\sigma_s > 0$ or $\sigma_s < 0$ should be used only for calculation.

3 CALCULATION OF VERTICAL VELOCITY Ω OF LOW-PRESSURE SYSTEMS

A low-pressure system is a small-scale vortex for which it is reasonable to select Eq.(16) for the purpose of discussion. L_x on the right-hand side of Eq.(16)

refers to radius R of the low-pressure system. When R , V , and σ_s are all constants, the right-hand side of Eq.(16) will be a known number. If we assume this number to be A , then

$$A = 0.02527 \frac{V}{R\sigma_s}$$

$$\frac{\omega}{1 + \omega} = A$$

$$\omega = \frac{A}{1 - A} \quad (17)$$

$$\omega = \frac{A}{1 - A} = \frac{0.02527 \frac{V}{R\sigma_s}}{1 - 0.02527 \frac{V}{R\sigma_s}} = \frac{0.02527V}{R\sigma_s - 0.02527V} \quad (18)$$

From the above equations, we can determine ω directly. The rotational updraft speed of a circular typhoon is at its maximum near the center of the cloud wall of the typhoon's eye and gradually decreases outwards. For most low-pressure systems, it is not possible to observe the low-pressure system eye, only the central axis. Airflow rises quickly around this axis and, similar to typhoons, the rotational updraft speed reaches its maximum near the central axis and gradually decreases outwards. Therefore, when Eq.(18) is used for calculating ω in low-pressure systems, the vertical velocity ω at different distances from the central axis must be determined. Taking a low-pressure system with $R = 1000$ m as an example, we can calculate the respective values of ω at positions 5, 10, 20, ...1000 m away from the central axis, i.e., set $R = 5, 10, 20, 30, \dots, 1000$ m, from which the distribution characteristics of ω inside the low-pressure system can be determined. Similarly, if the radius of the low-pressure system is only 50 m, it is only necessary to determine the values of ω at positions 5, 10, 20, 30, 40, and 50 m away from the central axis, i.e., set $R = 5, 10, 20, 30, 40, \text{ and } 50$ m.

According to the expression $\omega = -\rho g w$, the value of ω in hPa/s can be converted into vertical speed W in m/s. To explore the vertical motion in low-pressure systems of different horizontal scales, we designed two w-nomogram diagrams for the variation of R from 5 to 1000 m (Fig.1) and from 10 to 1000 km (Fig.2). The nomogram diagram provides a visual framework for comparing vertical and horizontal velocities in low-pressure systems of different scales or at different radii in the same low-pressure system.

Figure 1 shows that the absolute value of vertical velocity increases with increasing horizontal velocity at 850 hPa. The correspondence between vertical and horizontal velocities is a common feature for every radius, although the slope of increase is quite different for different radii. For example, if the horizontal velocity increases to 10 m/s, the vertical velocity will

increase to 2.37 m/s at 10 m, whereas it will only increase to 0.0243 m/s at 1000 m (about one-hundredth of 2.37 m/s). The rate of increase of vertical velocity associated with increasing horizontal velocity is found to decline with increasing radius. Generally, vertical velocity is larger near the center of a low-pressure system and decreases as it moves further away. In other words, vertical velocity increasingly intensifies with reducing horizontal scale of the low-pressure system.

Figure 2 is the same as Fig.1, but for radii varying from 10 to 1000 km. If the horizontal scale of the low-pressure system is >5 km, the vertical velocity will be reduced by two orders of magnitude, i.e., the measurement unit of vertical velocity will change from m/s to cm/s. In particular, if the radius of the low-pressure system is >1000 km, no matter how intense the horizontal velocity, the vertical velocity will barely exceed a few cm/s.

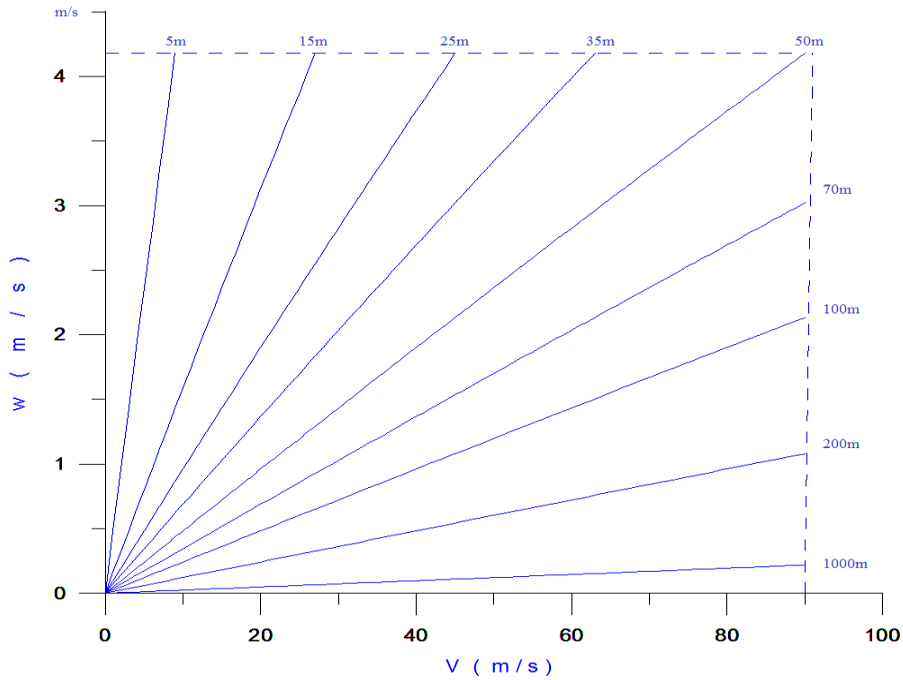


Figure 1. Nomogram of vertical speed (ω) and horizontal speed (V) of low-pressure systems with radii of 5–1000 m under 850 hPa.

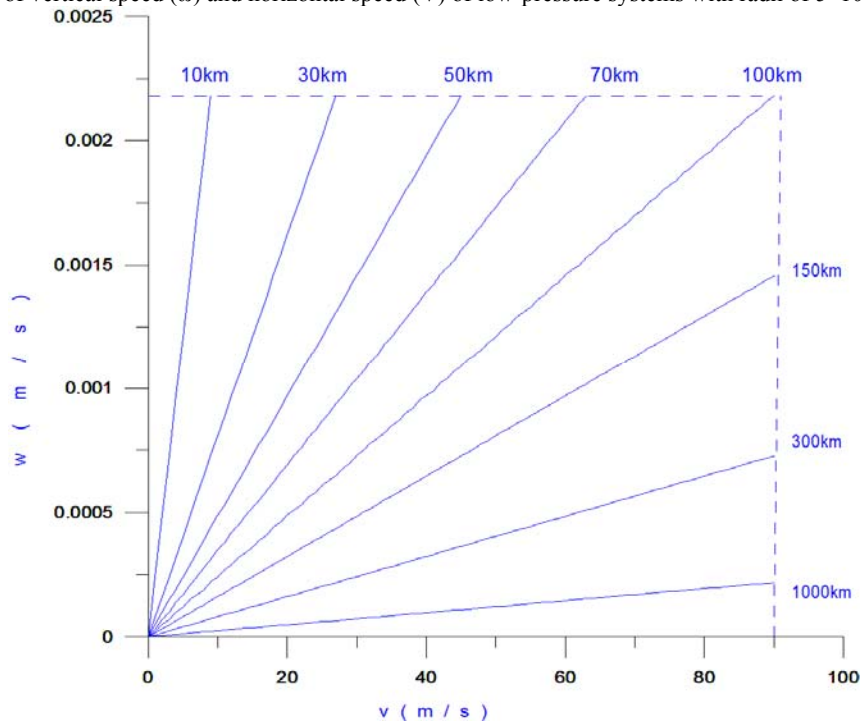


Figure 2. Same as Fig.1 but with radii of 10–1000 km.

Vertical velocity at about 850 hPa (approximately the bottom of cumulonimbus clouds) is higher relative to that at ground level and reaches its maximum in the mid-troposphere at about 500–400 hPa. Tables 1, 2, and 3 show the vertical velocities for horizontal wind speeds of 20, 40, and 80 m/s, respectively, with respect to ground level (1000 hPa), the height of cumulonimbus clouds (850 hPa), and mid-troposphere (500 hPa).

Table 1 shows that in the center of the low-pressure system at radius 10 m, the vertical wind speed of 3 m/s at ground level increases to about 11 m/s in the mid-troposphere, a nearly three-fold increase. This higher vertical velocity is expected to produce a considerable suction effect.

Table 2 shows the distribution of vertical velocity for a horizontal wind speed that is twice that shown in Table 1. Correspondingly, at different levels and different radii, vertical velocities are also about twice as those shown in Table 1.

When the horizontal wind speed is increased to 80 m/s, the ground level vertical velocity 10 m from the central axis is about 11 m/s, increasing to about 36

m/s in the mid-troposphere, showing an increase of 25 m/s. Therefore, the role of this difference in velocity in generating suction cannot be ignored, as evidenced by the ability of small-scale tornadoes to tear up trees and destroy houses. Notably, the horizontal wind speed of a tornado might be even greater than the example discussed here.

From a comparison of Figs. 1 and 2 and Tables 1–3, the following features can be observed.

1. For the same horizontal wind speed, larger-scale low-pressure systems have smaller vertical velocities, e.g., a reduction in scale by 10 times leads to a corresponding increase in vertical velocity;

2. For a low-pressure system of a certain scale, an increase in the horizontal wind speed leads to an increase in the vertical velocity, e.g., doubling the horizontal wind speed also doubles the vertical velocity;

3. For a low-pressure system of a certain scale with a certain horizontal wind speed, vertical velocity increases with height, reaching a maximum in the mid-troposphere.

Table 1. Distribution of vertical velocity (m/s) for a horizontal wind speed of 20 m/s at different height and radii.

R	10 m	50 m	100 m	1000 m	10 km	100 km	1000 km	4000 km
1000 hPa	3.0384	0.62673	0.3146	0.0316	0.0032	0.00032	0.00003	0.00001
850 hPa	4.61842	0.96066	0.48274	0.04849	0.00485	0.00049	0.00005	0.00002
500 hPa	10.91275	2.31868	1.16845	0.11768	0.01178	0.00118	0.00012	0.00003

Table 2. Same as Table 1 but for a horizontal wind speed of 40 m/s.

R	10 m	50 m	100 m	1000 m	10 km	100 km	1000 km	4000 km
1000 hPa	5.85453	1.24372	0.62673	0.06312	0.00632	0.00063	0.00006	0.00002
850 hPa	8.81287	1.90228	0.96066	0.09694	0.00970	0.00097	0.00010	0.00003
500 hPa	20.33329	4.56616	2.31868	0.23517	0.02355	0.00236	0.00024	0.00006

Table 3. Same as Table 1 but for a horizontal wind speed of 80 m/s.

R	10 m	50 m	100 m	1000 m	10 km	100 km	1000 km	4000 km
1000 hPa	10.91060	2.44936	1.24372	0.12614	0.01263	0.00126	0.00013	0.00003
850 hPa	16.14374	3.73063	1.90228	0.19368	0.01940	0.00194	0.00019	0.00006
500 hPa	35.77473	8.86025	4.56616	0.46959	0.04709	0.00471	0.00047	0.00012

Case study On May 20, 2013, a destructive low-pressure system touched down in Oklahoma (USA), which the National Weather Service evaluated as a category EF-5. The wind speed on the ground was 90 m/s and its radius was around 1000 m; the low-pressure system persisted for 40 min. According to Eq.(18), the updraft speed would have exceeded 12.1 m/s at a radius of 10 m near the ground and

exceeded 17.8 m/s at the base of the cumulonimbus cloud (around 850 hPa). The horizontal speed was more than twice that of a Level-12 hurricane, the vertical velocity was greater than twice that of a Level-8 hurricane, and the low-pressure system was extraordinarily destructive. The mid-tropospheric (500 hPa) vertical velocity was 39.07 m/s, i.e., 27 m/s greater than that at ground level. Many American

meteorologists have used the real-time monitoring data from this low-pressure system and concluded that the destructive power it released was more than eight times that of the Hiroshima atomic bomb. The town of Moore in the suburbs of Oklahoma was nearly completely destroyed (Chao^[9]).

The ω diagnostic equation for low-pressure systems, derived from the quasi-geostrophic ω -equation, is as shown below:

$$\omega = \frac{0.02527V}{R\sigma_s - 0.02527V}$$

From this equation, the following can be inferred:

(1) For stability σ_s , the vertical velocity ω is determined only by radius R and wind speed V (correlated positively with wind speed and negatively with radius).

(2) Vertical velocity ω increases gradually closer to the central axis.

(3) Vertical velocity ω increases with increasing horizontal speed.

(4) The low-pressure system radius and vertical velocity ω increase with increasing height.

(5) Irrespective of the horizontal speed, the maximum near-ground vertical velocity W of a low-pressure system is 80 m/s, and W will not exceed 100 m/s at the base of a cumulonimbus cloud under 850 hPa.

REFERENCES:

[1] ZHANG Jie. Small and Medium Scale Synoptic

Meteorology [M]. Beijing: China Meteorological Press, 2006: 242-244 (in Chinese).

[2] LV Mei-zhong, HOU Zhi-ming, ZHO U-yi. Dynamic Meteorology [M]. Beijing: China Meteorological Press, 2004: 142-202 (in Chinese).

[3] XU Feng, XIAO Yi-qing, LI Bo, et al. A tornado wind field characteristics of CFD numerical simulation [J]. Acta Aerodyn Sinica, 2013, 32(3): 103-115 (in Chinese).

[4] CHU Yan-Li, WANG Zhen-hui, RAN Ling-kun, et al. Typhoon Morakot (2009) in the process of rainstorm potential shear deformation wave action density diagnostic analysis and forecast application [J]. Acta Phys Sinica, 2013, 35(9): 89-95 (in Chinese).

[5] SONG Xiao-Jiang, XING Jian-yong, WANG Zhang-gu. A strong gustiness Bohai diagnosis analysis of the thunderstorm weather process [J]. Marine Forecasts, 2013, 25(2): 117-119 (in Chinese).

[6] ZHENG Feng, XIE Hai-hua. A tornado of nearly 30 years research progress in our country [J]. Meteorol Sci Technol, 2010, 32(3): 112-115 (in Chinese).

[7] KUAI L, HAAN F L, GALLUS W A, et al. CFD simulations of the flow field of a laboratory-simulated tornado for parameter sensitivity studies and comparison with field measurements [J]. Wind Struct, 2008, 43(3): 12-15.

[8] ALEXANDER C R, WURMAN J. The 30 may 1998 Spencer, south Dakota, storm. Part I: The structural evolution and environment of the tornadoes [J]. Mon Wea Rev, 2005, 22(3): 117-119.

[9] CHAO Lun. Hundreds of people and the disastrous tornado hit the United States [J]. Ecolg Econ, 2013, 7: 9-11 (in Chinese).

Citation: QU Wei-zheng, FAN Ting-ting and DU Ling. The low-pressure system in the vertical velocity omega on the scale of system sensitivity [J]. J Trop Meteorol, 2015, 21(S1): 66-72.